CSIRO PUBLISHING

International Journal of Wildland Fire
https://doi.org/10.1071/WF17031

A LiDAR-based analysis of the effects of slope, vegetation density, and ground surface roughness on travel rates for wildland firefighter escape route mapping

Michael J. Campbell[A,C], *Philip E. Dennison*[A] *and Bret W. Butler*[B]

[A]Department of Geography, University of Utah, 332 S 1400 E, Salt Lake City, UT 84112, USA.
[B]Rocky Mountain Research Station, USDA Forest Service, 5775 US Highway 10 W, Missoula, MT 59808, USA.
[C]Corresponding author. Email: mickey.campbell@geog.utah.edu

Abstract. Escape routes are essential components of wildland firefighter safety, providing pre-defined pathways to a safety zone. Among the many factors that affect travel rates along an escape route, landscape conditions such as slope, low-lying vegetation density, and ground surface roughness are particularly influential, and can be measured using airborne light detection and ranging (LiDAR) data. In order to develop a robust, quantitative understanding of the effects of these landscape conditions on travel rates, we performed an experiment wherein study participants were timed while walking along a series of transects within a study area dominated by grasses, sagebrush and juniper. We compared resultant travel rates to LiDAR-derived estimates of slope, vegetation density and ground surface roughness using linear mixed effects modelling to quantify the relationships between these landscape conditions and travel rates. The best-fit model revealed significant negative relationships between travel rates and each of the three landscape conditions, suggesting that, in order of decreasing magnitude, as density, slope and roughness increase, travel rates decrease. Model coefficients were used to map travel impedance within the study area using LiDAR data, which enabled mapping the most efficient routes from fire crew locations to safety zones and provided an estimate of travel time.

Additional keywords: firefighter safety, evacuation, travel efficiency, remote sensing, GIS.

Received 11 February 2017, accepted 20 July 2017, published online 27 September 2017

Introduction

Wildland firefighter escape routes are pre-planned routes firefighters take to move to a safety zone or other low-risk area (National Wildfire Coordinating Group 2016). Escape routes are an essential component of the Lookouts, Communications, Escape Routes, and Safety Zones (LCES) system and 10 standard firefighting orders for firefighter safety planning (Gleason 1991; Ziegler 2007). They should be established in advance of firefighting, known to all members of a fire crew, and re-evaluated as conditions change throughout the day (National Fire Protection Agency 2011). The goal in selecting escape routes is to determine the path of least resistance and lowest risk between fire crew location and safety zone. To maintain a margin of safety (Beighley 1995), firefighters must have a keen awareness of both fire behaviour and their own ability to traverse a given landscape. There is an extensive body of literature and several well established tools for modelling fire behaviour (e.g. Finney 2004; Finney 2006; Andrews 2014), and some data on fire crew physiological performance (Ruby *et al.* 2003). However, few studies have explored the interaction between landscape conditions and escape-route travel.

There are several landscape conditions that can affect travel rate in a wildland environment, including terrain slope (henceforth, 'slope'), low-lying vegetation density ('density') and ground surface roughness ('roughness'). Of these factors, slope has been the most extensively studied for its effects on travel rate. Butler *et al.* (2000) examined the effects of slope on travel rate using data from two fires with significant firefighter fatalities, South Canyon and Mann Gulch. Alexander *et al.* (2005) performed experiments with Alberta firefighters to determine the effects of not only slope, but also vegetation type, load carriage and trail improvement on travel rates. Tobler's Hiking Function (THF) is an empirically derived model for estimating travel rates based on slope (Tobler 1993) that has been widely used in a variety of contexts, including urban evacuation modelling (Wood and Schmidtlein 2012), outdoor recreation planning (Pettebone *et al.* 2009) and historical migration simulation (Kantner 2004), but has rarely been applied to the wildland firefighting environment, one exception being Fryer *et al.* (2013). Another common slope-travel rate function is Naismith's Rule, developed in 1892 by Scottish mountaineer William Naismith, which states that hiking 1 flat mile (~1600 m) should take 20 min with an additional 30 min for every 1000 feet (~300 m) of elevation gain, though it does not account for downhill travel (Norman 2004). More recently, Davey *et al.* (1994) derived a function based on a series of treadmill experiments that predicts sustainable uphill travel rates over long distances based on a baseline travel rate on flat slopes. Though mathematically similar to Naismith's Rule and THF, the function of Davey *et al.* (1994) provides a flexible framework for adjusting to individual-level fitness. Studies that have quantified slope effects on travel rate universally demonstrate that travelling up and down steep slopes reduces travel rate. However, methodological differences make it difficult to compare experimental data relevant to firefighter evacuation (e.g. Alexander *et al.* 2005) to models like THF, Naismith's Rule and Davey *et al.* (1994). Given the importance of slope as a predictor of travel rate, and the importance of travel rate on the effectiveness of escape routes, continued study is essential.

Few studies have examined the effects of vegetation and ground surface conditions on travel rates. Alexander *et al.* (2005) compared experimentally derived travel rates to a range of vegetation types, as categorised by Canadian Fire Behaviour Prediction fuel type. Taller, denser spruce (*Picea* spp.) and lodgepole pine (*Pinus contorta*) fuel types resulted in slower travel rates than shorter, less dense grass and slash fuel types. Anguelova *et al.* (2010) modelled pedestrian evacuation due to a wildfire using a qualitative, heuristic approach to characterise the effects of common vegetation types in Southern California on relative travel rates. However, the use of categorical fuel and vegetation types in these studies limits applying these relationships on a broad scale. No studies to date have explored the effects of roughness on escape route travel explicitly, but research in the field of applied physiology has produced relevant results. The Pandolf equation is a function for estimating the metabolic cost of travelling across various types of terrain and land cover, using a variety of 'terrain factors' first introduced by Soule and Goldman (1972), which are categorical multiplicative factors used for estimating energy expenditure including blacktop road (1.0), dirt road (1.1), light brush (1.2), heavy brush (1.5), loose sand (2.1) and soft snow (2.5) (Pandolf *et al.* 1976). Schmidtlein and Wood (2015) used these terrain coefficients to model evacuation times in the event of a tsunami, but point out how their categorical nature does not easily translate to more commonly used measures of land cover and highlight the importance of continued study to determine the degree to which such coefficients match reality.

Two fatality events, the 1994 South Canyon fire and the 2013 Yarnell Hill fire, highlight the critical effect that slope, density and roughness can have on travel rates. On the South Canyon fire, firefighters perished when trying to outrun flames up rocky slopes as steep as 55% (29°) in an area dominated by dense Gambel oak and pinyon–juniper woodlands (Butler *et al.* 2000). On the Yarnell Hill fire, firefighters were entrapped as they travelled along an escape route through terrain characterised by boulders and covered with thick chaparral brush (Arizona State Forestry Division 2013).

To maximise the effectiveness of escape routes, we need to deepen our understanding of how slope, density and roughness affect travel rate in a precise, quantitative manner. These three landscape conditions can all be readily modelled using airborne light detection and ranging (LiDAR) data. LiDAR is a type of active remote sensing system in which pulses of laser light are emitted from an airborne platform towards the earth's surface and reflected back to the sensor, the timing of which enables the precise measurement of three-dimensional ground and aboveground structure (Lefsky *et al.* 2002). Airborne LiDAR has been used extensively for mapping terrain (e.g. Kraus and Pfeifer 2001; Reutebuch *et al.* 2003), vegetation structure (e.g. Bradbury *et al.* 2005; Hudak *et al.* 2008) and roughness (e.g. Glenn *et al.* 2006; Sankey *et al.* 2010). As such, the use of LiDAR has great potential for mapping escape routes. However, in the absence of a complete understanding of how these landscape conditions affect travel, the effectiveness of such an approach is limited. Accordingly, the objectives of this study are to: (1) perform an experiment to test the effects of slope, density and roughness on travel rates, and (2) use the resulting data to develop a LiDAR-based geospatial model for optimising firefighter escape routes and estimating travel time to safety on a spatial scale most useful for wildland firefighting operations.

Methods

For this study, an airborne LiDAR dataset spanning Utah's Wasatch Front was obtained from the OpenTopography LiDAR data portal (opentopography.org). The data were acquired by Watershed Sciences, Inc. on behalf of the State of Utah between October 2013 and May 2014 and have an average point density of 11.93 points m^{-2}. The data are reported to have a respective average vertical accuracy of ±2.43, ±3.68 and ±5.41 cm in hard surface, shrub and forested areas. A subset of the broader Wasatch Front dataset within Levan Wildland Management Area (39°35′15″N, 111°49′56″W) was chosen as the study area based on diversity of topography and vegetation, public land ownership, and road accessibility (Fig. 1). Elevations range between 1650 and 1775 m with dominant vegetation types of Utah juniper (*Juniperus osteosperma*) woodlands, big sagebrush (*Artemisia tridentata*) shrublands and mixed perennial grasslands.

To test the effects of slope, density and roughness on travel rates, an experiment was conducted in which volunteer study participants were timed as they walked a series of linear transects. Twenty-two 100-m transects were placed to capture a range of vegetation and topographic conditions (Fig. 1). They were selected from a randomly generated set of transects to minimise within- and maximise between-transect landscape condition variability. Transects were established in the field using a Trimble Geo 7X GPS (Trimble, Inc., Sunnyvale, CA, USA, www.trimble.com/Survey/Trimble-Geo-7x.aspx, accessed 13 September 2017) with ≥200 point averaging for transect start and end points and a Laser Technology TruPulse 360 rangefinder (Laser Technology, Inc., Centennial, CO, USA, www.lasertech.com, accessed 13 September 2017) for azimuth and distance measurements. Sign posts were placed at each transect start and end, and coloured flagging was placed in between at intervals of ~5–10 m, depending on visibility.

There were 31 study participants, none of whom had previously worked as firefighters (Table 1). Participants were partnered together and each individual walked the transects twice, once in each direction, and timed themselves as they walked, from which travel rates were computed. Participants walked the numbered transects in sequential order, but to avoid the potentially confounding effects of fatigue, partner groups were each

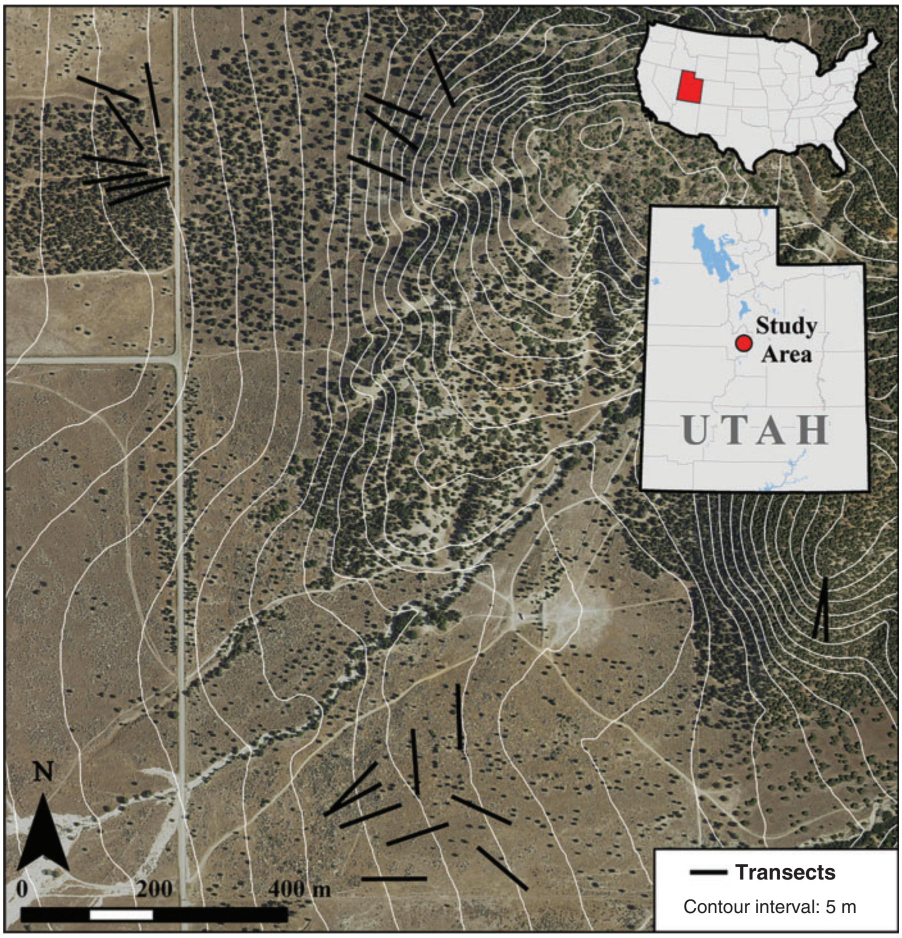

Fig. 1. Study area map, with background imagery care of ESRI (ESRI Inc., Redlands, CA, USA, www.esri.com).

Table 1. Study participant summary

	n	Mean age (years)	Mean height (m)	Mean weight (kg)	Mean exercise (h week^{-1})
All subjects	31	26.97	1.76	73.22	7.00
Male	19	26.11	1.81	81.65	7.78
Female	12	28.33	1.67	59.87	5.83

assigned different starting transects. The experiment took place over 2 days, each lasting ~6 h, with a 30-min lunch break in the middle of the day. Participants were additionally allowed to rest while their partner was walking the transect. Given that individuals have different average walking rates (e.g. because of different fitness levels, heights, weights, gaits), participants were asked to maintain a consistent level of effort when walking each transect. Additionally, participants were asked to stay as close to the flagged transect centreline as possible except when it intersected impassable vegetation, in which case participants were permitted to walk around obstacles.

Travel rates were compared with LiDAR-derived estimates of slope, roughness and density. These metrics were generated for each transect using a combination of *LAStools* LiDAR processing software (radpidlasso GmbH, Gilching, Germany, www.rapidlasso.com), ESRI *ArcGIS* geospatial software (ESRI Inc., Redlands, CA, USA, www.esri.com, accessed 13 September 2017), and R statistical software (R Core Team, Vienna, Austria, www.r-project.org, accessed 13 September 2017). LiDAR data were first classified into 'ground' and 'non-ground' points, using the *lasground* algorithm (Isenburg 2015). Several iterative classifications were performed, adjusting algorithm parameters as needed until the classification was deemed satisfactory according to a careful visual interpretation and comparison of the resulting classified LiDAR point cloud to high-resolution aerial imagery. Although no field validation was performed to obtain a quantitative, point-level accuracy assessment, it is likely that misclassifications between very low-lying non-ground points and ground points occurred. Slope was calculated by first creating a digital terrain model (DTM) at a spatial resolution of 1 m using the *las2dem* algorithm. For each transect (t), average slope (s) was then computed in degrees according to the difference in elevation in metres (e) at the start (a) and end (b) of each transect and the horizontal distance in metres (h) between a and b, such that:

$$s_t = \tan\left(\frac{e_b - e_a}{h}\right) \tag{1}$$

Roughness was calculated following an approach similar to that of Glenn *et al.* (2006) as the difference between a fine-scale DTM (0.25-m spatial resolution) and a 'smoothed' DTM (also 0.25 m) generated by calculating a focal mean of elevation values within a 2.5-m-radius circular kernel. The resulting raster dataset contained pixel values representing local deviations (e.g. bumps, pits) from the broader topography (Fig. 2). Linear transects were buffered by 5 m and the absolute values of the roughness raster data were averaged within each buffer to obtain a transect-level roughness in metres.

As vegetation density in different portions of the vertical canopy profile will have different effects on travel rates, it was first necessary to determine a suitable range of aboveground heights that would most directly affect travel. For example, very dense vegetation in a very high or very low height stratum will likely have little effect on travel rates, as one could readily traverse under or over the vegetation unimpeded. LiDAR point clouds can be used to estimate vegetation density in distinct height strata by calculating normalised relative point density (NRD). NRD is a calculation of the relative proportion of point returns that fall within a given height range as compared with the total number of points that fall within and below that height range, such that:

$$NRD_{ij} = \frac{\sum_i^j n}{\sum_0^j n} \tag{2}$$

where n is the number of LiDAR point returns, i is the floor (low value) of the height range and j is the ceiling (high value) of the height range (USDA Forest Service 2014). To calculate NRD, aboveground height for each non-ground LiDAR point was first calculated using the *lasheight* algorithm, which uses the ground points to generate a triangulated irregular network (TIN) representing the ground surface, and then computes the height of each non-ground point above the TIN surface. Transects were buffered by 5 m, and the point cloud was extracted within the buffer area. Eqn 2 was then used to calculate a single NRD value for the entire transect. Fig. 3 depicts an example height range along a

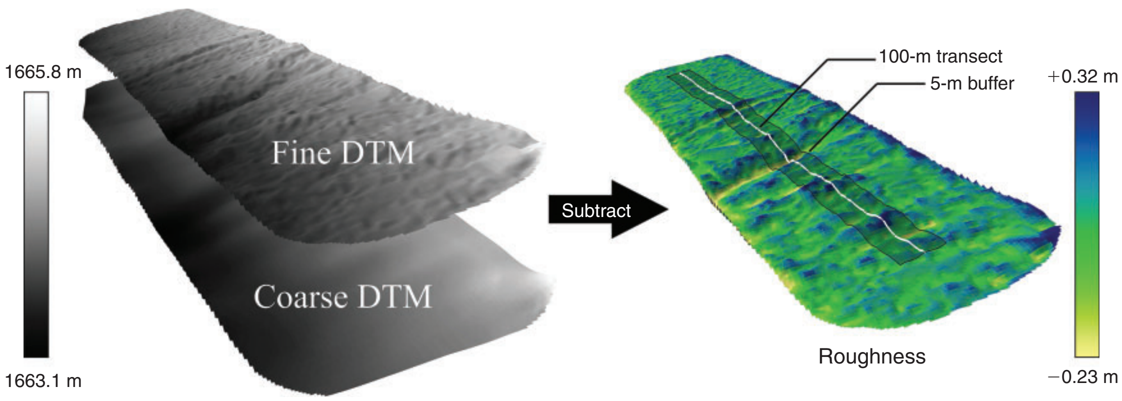

Fig. 2. Roughness calculation; digital terrain model (DTM) elevation values exaggerated 3× to highlight texture.

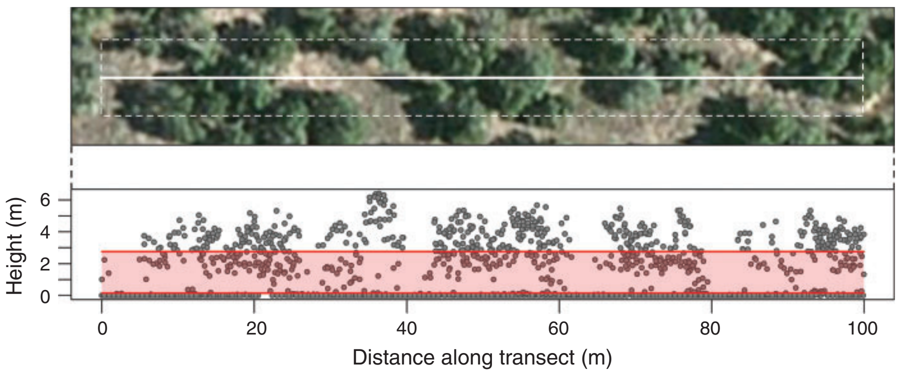

Fig. 3. Example transect with associated light detection and ranging (LiDAR) point cloud cross-section and example height range (0.15–2.75 m); heights scaled for clarity, with background imagery care of ESRI (ESRI Inc., Redlands, CA, USA, www.esri.com).

100-m transect, where $i = 0.15$ m and $j = 2.75$ m. NRD values range from 0 to 1, with 1 being indicative of very dense vegetation in a given height range and 0 representing very little or no vegetation.

In order to determine the height range that had the most significant effect on travel rates, a series of linear mixed effects regression (LMER) analyses were performed. As stated earlier, some study participants consistently walk faster than others regardless of landscape conditions, and, although this is potentially useful information, of primary interest are the *relative* effects (i.e. how much does vegetation density reduce travel rate independent of individual performance?). LMER modelling fits a series of models with variable (or, 'random') y-intercepts, providing an account of the fixed effects (the underlying trend) and the random effects (variability caused by individuals).

Two different LMER analyses were run using travel rate as the dependent variable. The first LMER analysis was designed to determine optimal NRD height range that best predicted travel rates. In order to minimise the confounding effects of slope, only data from transects with slopes of less than 5° ($n = 16$) were used in this analysis. For every possible contiguous height range between 0 and 5 m, at intervals of 5 cm, a LMER model was generated in R using the *lme4* package (Bates *et al.* 2015) to test the predictive power of NRD on travel rates and assessed for model fit. Models were assessed for fit using Nakagawa and Schielzeth (2013)'s measures for marginal and conditional R^2 (henceforth R^2_{m} and R^2_{c}), representing variance explained by the fixed effects and the variance explained by both the fixed and random effects respectively as implemented in *R* using the *MuMIn* package (Bartoń 2016). NRD for the height range that was able to best predict travel rates was selected for further use throughout the study as a representation of density.

The second LMER analysis assessed the combined effects of slope, density, and roughness on travel rates, again accounting for variability individuals' travel rates. The best-fit fixed effects LMER model took the form:

$$\text{travel rate} = \alpha + \beta_1\text{density} + \beta_2\text{roughness} + \beta_3\text{slope} + \beta_4\text{slope}^2 \quad (3)$$

where α is the y-intercept, representing travel rate for zero density, roughness and slope, and β are multiplicative model coefficients, representing relative effects of the landscape variables on travel rates. In order to use these travel impedance model coefficients derived from transect-level experimentation in a landscape-level geospatial model for escape route optimisation, each of the three landscape variables was computed on a per-pixel basis across the entire study area at a 5-m spatial resolution. Rasterised landscape variables were then multiplied by their model coefficients to derive travel impedance raster data throughout the study area. A route optimisation analysis was then performed in *R* using the *raster* and *gdistance* packages (Hijmans 2015; van Etten 2015). The *gdistance* package uses transition matrices to calculate the relative resistance of moving between eight directionally adjacent cells in a raster dataset. For each of the landscape conditions of interest, a transition matrix was generated such that for each cell, a travel cost (s) was computed for travelling to each of its adjacent cells, according to the LMER model coefficients (β_1, β_2, β_3 and β_4 above). The transition matrices were combined to enable an analysis of travel time for travelling between any two locations throughout the study area. Lastly, a series of simulations were performed to create escape routes between simulated fire crew and safety zone locations. Each route was generated automatically to identify the fastest route to safety, according to the combined transition matrix, using Dijkstra's algorithm (Dijkstra 1959). Dijkstra's algorithm computes the relative travel impedance of all possible routes from origin to destination based on a defined set of nodes (raster cells) and paths between them (connections between adjacent cells) and identifies the single, most efficient path.

Results

Fig. 4 depicts the three landscape parameters of interest (slope, density, and roughness) throughout the study area with the 22 transects overlaid to highlight the range of conditions captured in the experiment. Slopes ranged from 0 to 39.4°, density (0.15–2.75 m) ranged from 0 to 100%, and roughness ranged from 0 to 0.4 m. The majority of the juniper woodlands were found on steeper slopes at higher elevations, with sagebrush and

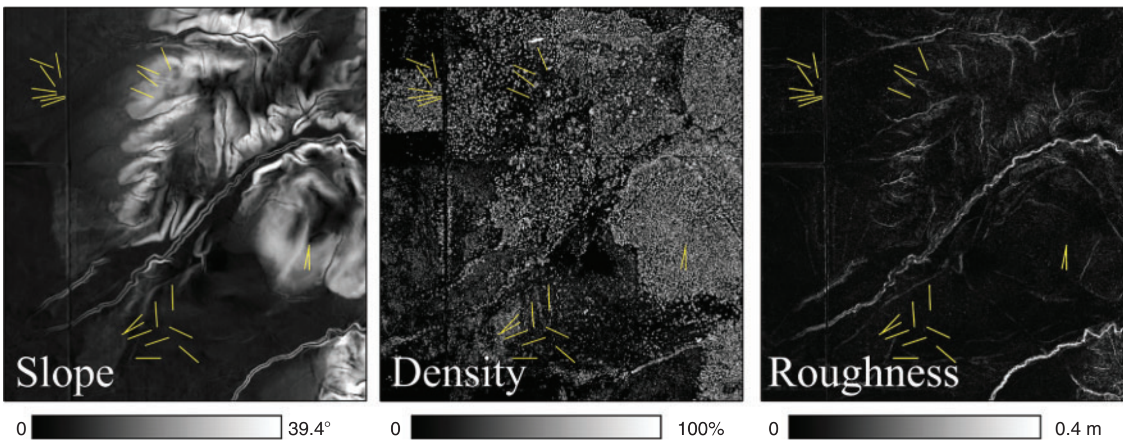

Fig. 4. Landscape parameters with transects.

grasslands dominating the lower-slope, lower-elevation terrain. In general, juniper woodlands tended to have the highest vegetation density, though a few of the sagebrush-dominant transects had higher vegetation densities (e.g. transects 15 and 16, Table 2). Roughness values were highest on steeper slopes and in dry streambeds, where erosional and depositional processes have created rocky ground surfaces.

In all, there were 1276 timed walks, with 10 subjects walking 22 transects, 19 subjects walking 20 transects, and two subjects walking 19 transects, all in both transect directions. All resultant travel rates were used in the subsequent analyses, with no outlier removal. The results of the first LMER analysis to determine the NRD height range that best predicted experimentally derived travel rates on slopes <5°, as approximated by R^2_m, can be seen in Fig. 5 and Table 3. Those height ranges with floors of 2 m or higher (e.g. 2–3 m, 3–4 m) had very little predictive power, indicating that vegetation solely above the heads of study participants (average height = 1.76 m) had little effect on travel rates. Conversely, those ranges with ceilings below 1 m (e.g. 0–0.5 m, 0–1 m) have low predictive power as well, suggesting that low-lying density alone does not account for much of the variability in travel rates. Consistently, the height ranges with floors between 0 and 0.5 m and ceilings between 2 and 4 m tend to be the best predictors of travel rates. Although several similar height ranges resulted in similarly high predictive power (Table 3), the single best height range of prediction was 0.15–2.75 m, with a R^2_m of 0.54 and R^2_c of 0.84 (Fig. 5). This range was used throughout the remaining analyses.

Fig. 6 highlights the fairly wide dispersal of travel rate values at each transect, as represented by the spread in the y direction at each x location. This spread represents the tendency for some individuals to travel faster than others regardless of landscape conditions, and was accounted for by using LMER.

Table 2. **Transect landscape parameter mean values**

Transect	Length (m)	Slope (°)	Density (%)	Roughness (m)
1	99.77	3.04	33.24	2.02×10^{-2}
2	99.96	3.55	25.17	1.91×10^{-2}
3	99.77	3.52	31.50	1.81×10^{-2}
4	99.80	3.71	16.83	1.78×10^{-2}
5	100.04	1.74	9.76	2.06×10^{-2}
6	100.07	3.29	3.57	2.18×10^{-2}
7	100.01	0.09	1.86	2.47×10^{-2}
8	100.20	15.23	4.75	2.61×10^{-2}
9	102.49	13.22	9.35	3.57×10^{-2}
10	99.70	14.61	17.87	2.16×10^{-2}
11	100.77	14.02	16.72	2.46×10^{-2}
12	99.97	2.60	4.08	1.64×10^{-2}
13	99.69	3.15	13.27	1.76×10^{-2}
14	99.99	2.07	19.94	1.97×10^{-2}
15	100.31	2.96	34.17	2.25×10^{-2}
16	100.48	2.16	34.65	1.89×10^{-2}
17	100.52	1.98	27.44	2.41×10^{-2}
18	100.51	0.44	13.79	2.18×10^{-2}
19	100.17	2.21	5.61	1.71×10^{-2}
20	99.95	1.61	2.98	1.80×10^{-2}
21	99.96	15.90	40.20	2.04×10^{-2}
22	100.06	15.57	30.47	1.83×10^{-2}

The second LMER analysis to determine the combined effects of slope, density, and roughness on travel rates took the following form ($R^2_m = 0.59$; $R^2_c = 0.82$):

$$travel\ rate = 1.662 - 1.076 \times density - 9.011 \times roughness - \left(5.191 \times 10^{-3}\right) \times slope - \left(1.127 \times 10^{-3}\right) \times slope^2 \quad (4)$$

Each of the landscape parameters had a significant ($P < 0.001$) negative effect on travel rates, suggesting that as slope, density and roughness increase, travel rates decrease (Table 4). Fig. 7 provides a visualisation of the fixed and random effects of each

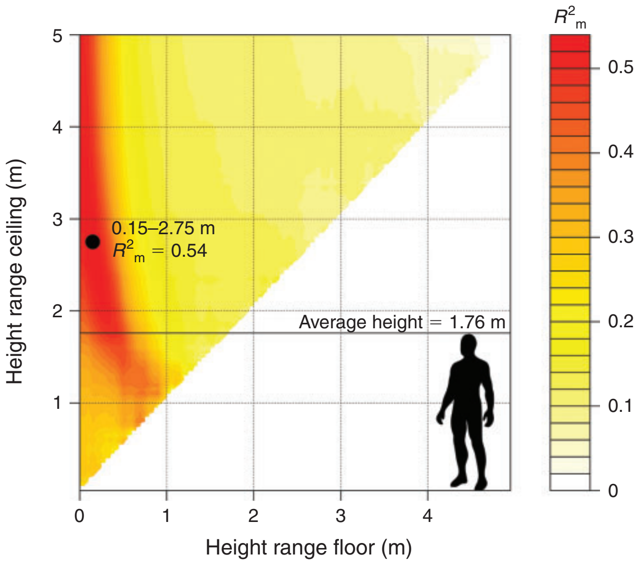

Fig. 5. Power of light detection and ranging (LiDAR) normalised relative point density (NRD) height ranges from 0 to 5 m for predicting travel rates along slopes of <5° as approximated by Nakagawa and Schielzeth (2013)'s measures for marginal and conditional R^2 (R^2_m) compared with average study subject height. Best interval (0.15–2.75 m) shown.

Table 3. **Results from regression analyses to determine optimal light detection and ranging (LiDAR) normalised relative point density (NRD) height range for predicting travel rate along slopes of less than 5°**

A total of 5053 NRD height ranges were tested, each representing a unique range between a floor and ceiling height. R^2_m and R^2_c are Nakagawa and Schielzeth (2013)'s measures for marginal and conditional R^2 representing variance explained by the fixed effects and the variance explained by both the fixed and random effects

Rank	NRD height range	R^2_m	R^2_c
1	0.15–2.75 m	0.540	0.839
2	0.15–2.70 m	0.540	0.838
3	0.15–2.65 m	0.539	0.838
4	0.15–2.60 m	0.539	0.837
5	0.15–2.80 m	0.539	0.837
…	…	…	…
5053	4.85–4.90 m	0.008	0.272

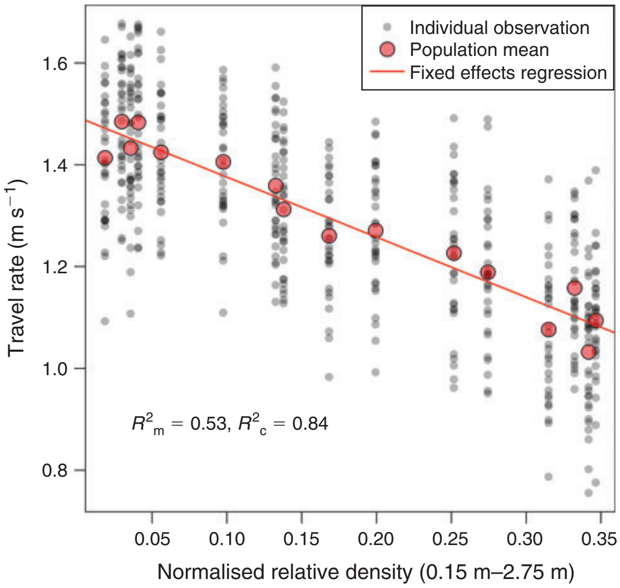

Fig. 6. Effect of density, as approximated by the optimal light detection and ranging (LiDAR) normalised relative point density (NRD) height range (0.15–2.75 m), on travel rates along slopes less than 5°.

Table 4. Fixed effects for model predicting travel rates

Probabilities are significant at: ***, α = 0.001. Residual degrees of freedom = 1269

Parameter	β	s.e.	$\beta_{standardised}$	t	P
intercept (α)	1.662	0.025			
density	−1.076	0.024	−0.551	−45.67	<0.001***
roughness	−9.011	0.743	−0.171	−12.13	<0.001***
slope	-5.191×10^{-3}	3.675×10^{-4}	−0.168	−14.12	<0.001***
slope^2	-1.127×10^{-3}	3.649×10^{-5}	−0.263	−30.89	<0.001***

landscape parameter. In order to display these relationships in two dimensions, for each landscape parameter (e.g. slope), the other two (e.g. density and roughness) were assumed to be the median value of those parameters among all of the transects. As can be seen from the magnitude of the standardised model coefficients ($\beta_{standardised}$, Table 4), and an analysis of variable-specific partial R^2_m, density had the greatest effect on travel rates, followed by slope and roughness.

Using the model coefficients from Table 4, Dijkstra's algorithm (Dijkstra 1959), as implemented in the *R gdistance* package (van Etten 2015) was performed to generate a series of simulated least-cost escape routes throughout the study area. Example resulting escape routes in Fig. 8 highlight the anisotropic effects of slope across this landscape, where the least-cost route from *a* to *b* differs from that of the reverse direction. Whereas the least-cost routes are actually longer than the straight-line distance between these two points, the travel time along the optimised routes were lower than the straight-line routes (Table 5). Similarly, whereas the *b* to *a* route was longer than the *a* to *b* route, the travel time from *b* to *a* is shorter.

A series of 1000 escape-route simulations was performed between randomly generated location pairs to illustrate the effects of landscape parameters on route designation (Fig. 9). Slope has a major effect on route placement, given the greater amount of route overlap in areas where slopes are low and the sparseness in steep areas. Density is more locally variable on the landscape, allowing for least-cost paths to traverse small avenues of comparably low density within broader swaths of dense vegetation. Roughness is inconsistently distributed throughout the study area, with sparse pockets of high roughness typically found in drainage channels bearing little apparent effect on the placement of escape routes. The straight north–south line with a high degree of escape route overlap that appears in the western portion of the study area is a road, highlighting the model's implicit bias towards low-slope, low-density and smooth surfaces.

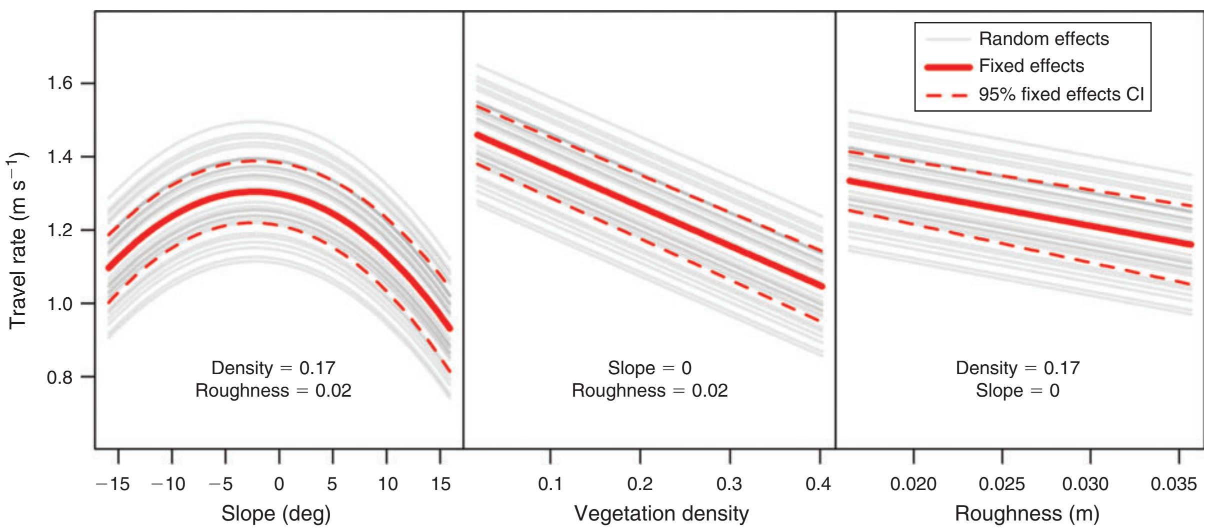

Fig. 7. Predicted results of linear mixed effects regression (LMER) for each landscape condition within the range of values found on transects throughout the study area, assuming a median value of the other two conditions.

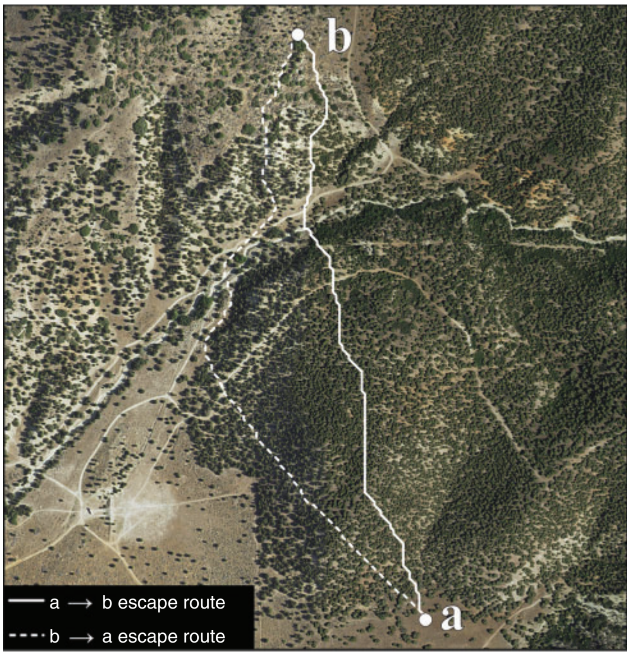

Fig. 8. Two simulated escape routes representing the least-cost paths between points *a* and *b* in both directions; background imagery: ESRI (ESRI Inc., Redlands, CA, USA, www.esri.com).

Discussion

This study examined the effects of slope, density and roughness on travel rates in order to develop a geospatial model for wildland firefighter escape route optimisation. It represents a valuable contribution to the existing body of research surrounding the effects of slope on travel rates, and a novel attempt at quantifying the effects of density and roughness. At present, escape routes are designated by firefighting personnel based on the recommendations of the National Wildfire Coordinating Group's Incident Response Pocket Guide, which suggest avoiding steep uphill escape routes, and scouting for loose soils, rocks, and vegetation (National Wildfire Coordinating Group 2014). Although these are important recommendations, the language is inherently subjective (e.g. 'steep', 'loose'), which can result in judgment error. This study introduces a standardised method for quantifying these variables and providing an experimentally derived account of their effects on travel. It also provides a framework for mapping travel rates across large areas, something that has not previously been possible. Provided that there are LiDAR data available within a given area, the resulting geospatial escape route optimisation model can be used as a decision support tool, providing fire crew members with objective insight to aid in the identification of efficient escape routes.

An important finding from this study was the determination of the aboveground density height range that most directly

Table 5. Resulting travel distances, times and rates for simulated escape routes

Route	Straight-line distance (m)	Route distance (m)	Travel time (s)	Straight line mean travel rate (m s^{-1})	Route mean travel rate (m s^{-1})
a → b	941.5	1038.9	969.6	0.97	1.07
b → a	941.5	1157.8	950.0	0.99	1.22

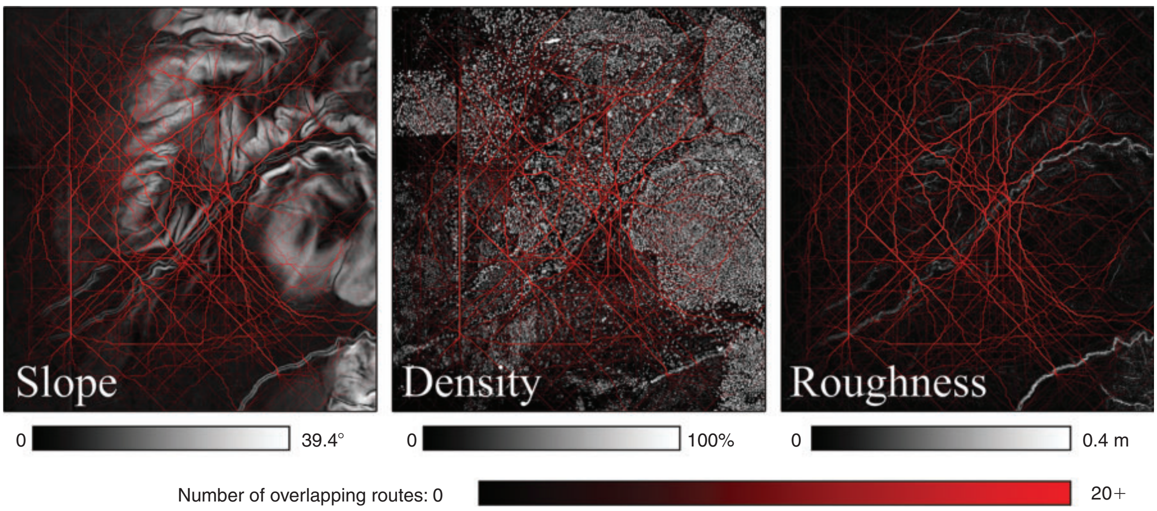

Fig. 9. Results of least-cost routes between 1000 randomly generated point location pairs throughout the study area with route overlap displayed against landscape parameters.

affected travel rates (0.15–2.75 m). The range floor (0.15 m) demonstrates that vegetation shorter than 15 cm in stature will most likely have little or no effect on one's ability to traverse a given landscape. The range ceiling, however, is nearly a meter taller than the mean height of study participants (1.76 m). Although we did not collected GPS data to track individual movement, anecdotal evidence gleaned from experimental observation suggested obstacle avoidance, rather than passage through obstacles, was a primary cause of travel rate reduction. Given the subjectivity associated with obstacle avoidance and individual route selection, it is possible that study participants tended to avoid vegetation slightly overhead based on perception of travel efficiency, even if passage under said vegetation would not greatly impede travel. It is also possible that the specific vegetation types found within the study area are partly responsible for the modelled importance of overhead vegetation. Particularly in the case of Utah juniper, the densest portion of the canopy lies between ~2 and 4 m in height (Fig. 10). It is likely that density in these higher portions of the canopy are highly correlated with density in the lower portions of the canopy as well. In other words, dense vegetation lying above the heads of study participants, although not directly affecting travel, likely indicates similarly dense vegetation at height ranges that do directly affect travel.

Although the 0.15–2.75-m height range was identified as the best range for predicting travel rates, as Table 3 highlights, there are several very similar ranges that possess similar predictive power. When combined with the inherent error in the ground point classification process and subtle LiDAR vertical inaccuracies, we can more broadly state that vegetation that generally occupies the same vertical space as a human (e.g. 0–3 m) most directly impedes travel.

This study has several assumptions and limitations that warrant further discussion. Perhaps the most important limitation is that the experiments were performed with non-firefighting personnel and without typical firefighting gear. That said, the test population was not entirely dissimilar to the firefighting community, demographically. According to the National Wildland Firefighter Workforce Assessment, almost 50% of aid- and tech-level USDA Forest Service firefighting personnel were between the ages of 26 and 35, as compared with the mean age of our study participants, which was 27 (USDA Forest Service 2010). Additionally, given the physical demands of the firefighting profession, firefighters tend to be of a high fitness level. By comparison, the study population was of generally above-average fitness, exercising a self-reported average of 7 h per week. One key difference is that this study population had a relatively large female population as compared with that of the firefighting community (39 *v.* 16% in the USDA Forest Service; USDA Forest Service 2010).

Regardless of the specific sample population used to derive the relative effects of landscape conditions, estimating travel rates should be done with great caution, particularly when simulating escape routes travel in a potentially dangerous wildfire environment. The most valuable contribution of this study is the analysis of *relative* effects of landscape conditions on travel rates, which are more robust to slight differences in individuals' heights, weights and fitness levels. Our data confirm this robustness, with an R^2_c value of 0.82, which suggests

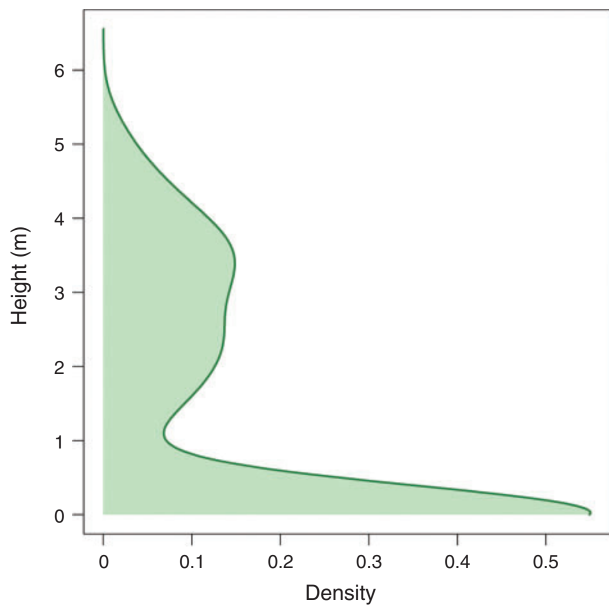

Fig. 10. Density plot of light detection and ranging (LiDAR) point return heights, measured as a proportion of all returns, for a transect with dense juniper.

that when accounting for the small differences in individual travel rate biases, 82% of the variance in overall travel rate is explained by slope, density, and roughness. The resulting model enables the automated generation of the fastest route to safety, irrespective of specific resulting travel rates and times.

It is worth noting that study participants walked, rather than ran, the transects. If subjects were asked to run the transects, the resulting between-subject variability would make a robust analysis much more difficult. Additionally, the effects of fatigue between running the first and last of 22 transects would be more pronounced than those of walking, making the within-subject variability problematic for modelling purposes. Although one might typically associate escape routes being a measure of last resort, the ideal escape route evacuation scenario is one in which a fire crew proceeds along an escape route in line at a controlled, walking pace. Although subjects were asked to maintain a consistent level of effort while walking transects, there remained a level of uncertainty in the computation of relative travel impedance due to a lack of quantitative control for energy expenditure levels. To further refine the relationship between landscape conditions and travel rates would require the collection of more robust measures of physical exertion, such as oxygen consumption rates, which was beyond the scope of our analysis. In addition, having subjects walk the same transects several times could have provided an estimate of uncertainty; however, given experimental time constraints, this would have limited the total number of transects and, by proxy, the range of landscape conditions tested. Fig. S1 in the Supplementary material provides a graphical depiction of the relative consistency of travel rates, according to how each study participant's travel rates ranked among all participants for each transect.

Another limitation of this study is the limited range of landscape conditions sampled throughout the 22 transects.

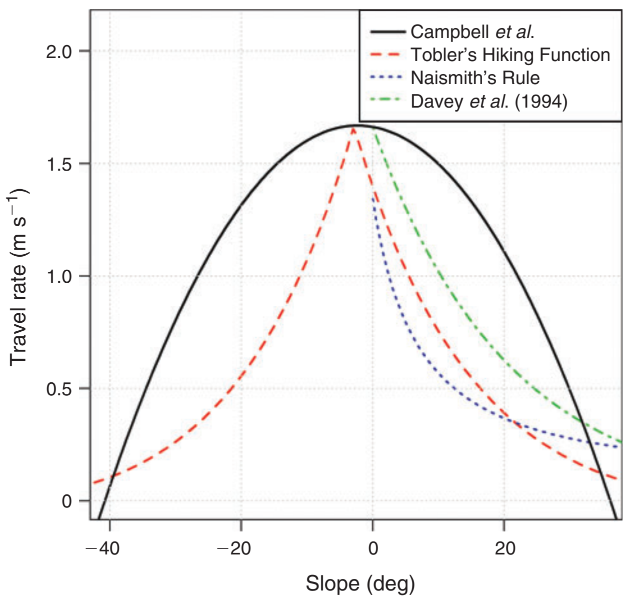

Fig. 11. Comparison of model results (calculated assuming zero vegetation density and zero ground surface roughness) to three well-established models used to estimate the effects of slope on travel rate. Davey *et al.* (1994)'s model was calibrated to match our model's 0° slope travel rate.

Although a wide range of conditions was captured, obtaining an exhaustive sample was impossible given the practical constraints of testing human subjects. This is particularly true of slope, where our maximum sampled slope was ~15°. As a result, we must extrapolate the effects on travel rates of slopes steeper than 15°, which may in reality take a different form than our proposed model. For example, THF, Naismith's Rule and Davey *et al.* (1994)'s function all flatten out towards the 'tails' on very steep slopes, but never quite reach a travel rate of zero, whereas our model calculates a travel rate of zero above slopes of ~36° and below slopes of ~−40° (Fig. 11). The model fit presented in Fig. 11 represents the effects of slope assuming zero density and roughness. As Fig. 11 depicts, the effects of slope as determined in our model are less pronounced than the other three models, likely due to differences in methodology. Whereas our study provides an account of the effects of slope over relatively short distances in wildland environments (100 m), the other three are based on long distance hiking on improved trails or treadmills.

The strength of the approach taken in this study lies in the broad applicability of LiDAR metrics tested. Regardless of geography, the quantitative measures that were computed from LiDAR data can be calculated in any environment. However, airborne LiDAR pulse density and overstorey vegetation conditions can have significant effects on the precision with which these measures are computed. The calculation of slope is fairly robust to these limitations, given the coarse scale of analysis. However, accurate estimation of understorey vegetation density and roughness relies on a sufficient amount of LiDAR pulse energy reaching the understorey and ground surface, requiring a balance between LiDAR pulse density and overstorey vegetation density. Though no sensitivity tests were performed to determine the effect of pulse density or overstorey conditions on characterising landscape conditions, it is likely that lower pulse densities or denser upper vegetation canopies than those in our study would reduce the effectiveness of our approach. The very nature of the roughness calculation we performed relies on assessing the difference between microtopography and macrotopography. As ground point densities decrease, those two measures begin to converge, reducing the ability to characterise small perturbations in the ground surface. Similarly, the understorey vegetation density calculation assumes that LiDAR pulse spacing will be sufficiently dense, so as to enable interaction with multiple features within the vertical canopy profile. With a much lower pulse density, deciphering between those points that reflect off of the top of the canopy and the middle of the canopy becomes much more difficult. Vegetation density, in particular, would also be difficult to characterise in vegetation types with very dense upper canopies, where relatively little airborne LiDAR pulse energy can reach the understorey. However, particularly in the fire-prone coniferous forests throughout the western United States, with comparably permeable upper canopies, this method should translate well.

A key assumption made in the development of this methodology is that the fastest route to safety is always the best route to safety, when in reality, this may not be the case. There are two key variables not assessed in our model: (1) road or trail access and (2) the location of the wildland fire. As Alexander *et al.* (2005) revealed, travelling along improved trails (flagged, cleared of brush) significantly reduced travel time along an escape route. Although this is implicitly accounted for in our model (presumably roads or trails have lower slope, density and roughness than off-trail areas), it is not explicitly built into the model. In a wildland firefighting environment, where high winds and smoke can greatly reduce visibility, travelling along a clearly defined road or trail could prove to be highly advantageous, even if slower than the 'optimal' route. That being said, by using a GPS and flagging the route identified by our algorithm, firefighters could reduce travel time by a potentially critical amount. Second, this model makes no attempt to characterise fire behaviour or identify current fire location. As such, it is conceivable that the fire would spread in a direction that would render the escape routes unsuitable or even fatal, as in the case of the Yarnell Hill fire in 2013. To address these points, future work could include model refinement to include an optional bias towards roads or trails and incorporation of fire location or a fire behaviour model, such as was done by Fryer *et al.* (2013) and Anguelova *et al.* (2010), to bias the model away from potentially dangerous routes.

Conclusions

The infusion of high resolution-high precision geospatial data, such as airborne LiDAR, into fire safety planning has the potential to greatly improve the consistency, reliability and efficiency of designating escape routes. However, escape routes are merely one component of the LCES system and must be connected to a safety zone or other low-risk area. As such, this research compliments recent work by Dennison *et al.* (2014) and Campbell *et al.* (2017), who have demonstrated methods for taking advantage of the advanced capabilities of LiDAR for safety zone identification and evaluation. Taken together, these methodologies can eliminate much of the potential for costly errors in the decision-making process when implementing LCES.

This study provides several important fire safety management implications:

- When designating escape routes, every attempt should be made to avoid steep slopes, dense vegetation, and rough ground surfaces.
- The use of airborne LiDAR to precisely quantify these landscape conditions can help select the most efficient escape routes.
- Mean walking travel rate on flat slopes, with minimal vegetation and ground surface roughness was 1.66 m s^{-1}.
- Travelling up slopes of 5, 10 and 15° reduced the travel rate by 3, 10 and 20% respectively.
- Travelling down slopes of 5, 10 and 15° reduced the travel rate by 0, 4 and 11% respectively.
- Travelling through dense juniper (NRD = 0.33) and dense sagebrush (NRD = 0.35) reduced the travel rate by 22 and 23% respectively.
- Travelling along rough ground surfaces (roughness = 3.57×10^{-2} m) reduced the travel rate by 19%.

Particularly in light of the push to collect nationwide LiDAR data throughout the United States within a decade as part of the USGS 3D Elevation Program (Snyder 2012), methods such as those presented in this study have the potential to enhance wildland firefighting safety. More work is certainly needed to validate and refine the results obtained in our experiments, and to test the additional effects of carrying packs, increased travel distance, and other external conditions such as temperature and humidity on firefighter travel rates, but this study represents a novel contribution in a direction that, as yet, has remained largely unexplored in the scientific and applied literature.

Conflicts of interest

The authors declare that they have no conflicts of interest.

Acknowledgements

Funding for this research was provided by the USDA Forest Service National Fire Plan through the Office of Research, the National Wildfire Coordinating Group Fire Behaviour Subcommittee, and the Wildland Fire Management Research Development and Application Program, Cooperative Agreements 14JV11221637123 and 15CR11221637105. We owe a great debt of gratitude to the volunteer study participants whose efforts enabled the success of the field experiment and to Dr Andrea Brunelle for her assistance in recruiting.

References

Alexander ME, Baxter GJ, Dakin GR (2005) Travel rates of Alberta wildland firefighters using escape routes. In 'Eighth International Wildland Fire Safety Summit', 26–28 April 2005, Missoula, MT, USA. (Eds BW Butler, ME Alexander) pp. 1–11. (International Association of Wildland Fire: Missoula, MT, USA)

Andrews PL (2014) Current status and future needs of the BehavePlus Fire Modeling System. *International Journal of Wildland Fire* **23**, 21–33. doi:10.1071/WF12167

Anguelova Z, Stow DA, Kaiser J, Dennison PE, Cova T (2010) Integrating fire behavior and pedestrian mobility models to assess potential risk to humans from wildfires within the US–Mexico border zone. *The Professional Geographer* **62**, 230–247. doi:10.1080/00330120903543756

Arizona State Forestry Division (2013) Yarnell Hill fire: serious accident investigation report. 23 September 2013. Available at http://wildfiretoday.com/documents/Yarnell_Hill_Fire_report.pdf [Verified 9 February 2017]

Bartón K (2016) MuMIn: multi-model inference. R package version 1.15.6. Available at http://CRAN.R-project.org/package=MuMIn [Verified 20 December 2016]

Bates D, Maechler M, Bolker B, Walker S (2015) Fitting linear mixed-effects models using lme4. *Journal of Statistical Software* **67**, 1–48. doi:10.18637/JSS.V067.I01

Beighley M (1995) Beyond the safety zone: creating a margin of safety. *Fire Management Notes* **55**, 22–24.

Bradbury RB, Hill RA, Mason DC, Hinsley SA, Wilson JD, Balzter H, Anderson GQ, Whittingham MJ, Davenport IJ, Bellamy PE (2005) Modelling relationships between birds and vegetation structure using airborne LiDAR data: a review with case studies from agricultural and woodland environments. *The Ibis* **147**, 443–452. doi:10.1111/J.1474-919X.2005.00438.X

Butler BW, Cohen JD, Putnam T, Bartlette RA, Bradshaw LS (2000) A method for evaluating the effectiveness of firefighter escape routes. In '4th International Wildland Fire Safety Summit', 10–12 October 2000, Edmonton, AB, Canada. (Eds BW Butler, KS Shannon) pp. 42–53. (International Association of Wildland Fire: Missoula, MT, USA)

Campbell MJ, Dennison PE, Butler BW (2017) Safe separation distance score: a new metric for evaluating wildland firefighter safety zones using LiDAR. *International Journal of Geographical Information Science* **31**, 1448–1466. doi:10.1080/13658816.2016.1270453

Davey RC, Hayes M, Norman JM (1994) Running uphill: an experimental result and its applications. *The Journal of the Operational Research Society* **45**, 25–29. doi:10.1057/JORS.1994.3

Dennison PE, Fryer GK, Cova TJ (2014) Identification of firefighter safety zones using LiDAR. *Environmental Modelling & Software* **59**, 91–97. doi:10.1016/J.ENVSOFT.2014.05.017

Dijkstra EW (1959) A note on two problems in connexion with graphs. *Numerische Mathematik* **1**, 269–271. doi:10.1007/BF01386390

Finney MA (2004) FARSITE: fire area simulator-model development and evaluation. USDA Forest Service, Rocky Mountain Research Station, Research Paper RMRS-RP-4. (Ogden, UT, USA)

Finney MA (2006) An overview of FlamMap fire modeling capabilities. In 'Fuels management—how to Measure Success: Conference Proceedings', 28–30 March 2006, Portland, OR, USA. (Eds PL Andrews, BW Butler) pp. 213–220. (USDA Forest Service, Rocky Mountain Research Station: Fort Collins, CO, USA)

Fryer GK, Dennison PE, Cova TJ (2013) Wildland firefighter entrapment avoidance: modelling evacuation triggers. *International Journal of Wildland Fire* **22**, 883–893. doi:10.1071/WF12160

Gleason P (1991) LCES – a key to safety in the wildland fire environment. *Fire Management Notes* **52**, 9.

Glenn NF, Streutker DR, Chadwick DJ, Thackray GD, Dorsch SJ (2006) Analysis of LiDAR-derived topographic information for characterizing and differentiating landslide morphology and activity. *Geomorphology* **73**, 131–148. doi:10.1016/J.GEOMORPH.2005.07.006

Hijmans RJ (2015). raster: geographic data analysis and modeling. R package version 2.5–2. Available at http://CRAN.R-project.org/package=raster [Verified 20 December 2016]

Hudak AT, Crookston NL, Evans JS, Hall DE, Falkowski MJ (2008) Nearest neighbor imputation of species-level, plot-scale forest structure attributes from LiDAR data. *Remote Sensing of Environment* **112**, 2232–2245. doi:10.1016/J.RSE.2007.10.009

Kantner J (2004) Geographical approaches for reconstructing past human behavior from prehistoric roadways. In 'Spatially Integrated Social Science: Examples in Best Practice'. pp. 323–344. (Oxford University Press: Oxford, UK)

Kraus K, Pfeifer N (2001) Advanced DTM generation from LIDAR data. *The International Archives of the Photogrammetry, Remote Sensing and Spatial Information Sciences* **34**, 23–30.

Lefsky MA, Cohen WB, Parker GG, Harding DJ (2002) LiDAR Remote Sensing for Ecosystem Studies LiDAR, an emerging remote sensing technology that directly measures the three-dimensional distribution of plant canopies, can accurately estimate vegetation structural attributes and should be of particular interest to forest, landscape, and global ecologists. *Bioscience* **52**, 19–30. doi:10.1641/0006-3568(2002)052[0019:LRSFES]2.0.CO;2

Nakagawa S, Schielzeth H (2013) A general and simple method for obtaining R^2 from generalized linear mixed-effects models. *Methods in Ecology and Evolution* **4**, 133–142. doi:10.1111/J.2041-210X.2012.00261.X

National Fire Protection Agency (2011) Firewise communities: firefighter safety in the WUI. Available at http://learningcenter.firewise.org/Firefighter-Safety/3-4.ph [Verified 20 December 2016]

National Wildfire Coordinating Group (2014) Incident response pocket guide. Available at http://www.nwcg.gov/sites/default/files/products/pms461.pdf [Verified 20 December 2016]

National Wildfire Coordinating Group (2016) Glossary A–Z. Available at http://www.nwcg.gov/glossary/a-z [Verified 20 December 2016]

Norman JM (2004) Running uphill: energy needs and Naismith's Rule. *The Journal of the Operational Research Society* **55**, 308–311. doi:10.1057/PALGRAVE.JORS.2601671

Pandolf KB, Givoni B, Goldman RF (1976) Predicting energy expenditure with loads while standing or walking very slowly. US Army Research Institute of Environmental Medicine Paper USARIEM-M-3/77. (Natick, MA, USA)

Pettebone D, Newman P, Theobald D (2009) A comparison of sampling designs for monitoring recreational trail impacts in Rocky Mountain National Park. *Environmental Management* **43**, 523–532. doi:10.1007/S00267-008-9261-9

Reutebuch SE, McGaughney RJ, Andersen HE, Carson WW (2003) Accuracy of a high-resolution LiDAR terrain model under a conifer forest canopy. *Canadian Journal of Remote Sensing* **29**, 527–535. doi:10.5589/M03-022

Ruby BC, Leadbetter GW III, Armstrong DW, Gaskill SE (2003) Wildland firefighter load carriage: effects on transit time and physiological responses during simulated escape to safety zone. *International Journal of Wildland Fire* **12**, 111–116. doi:10.1071/WF02025

Sankey JB, Glenn NF, Germino MJ, Gironella AIN, Thackray GD (2010) Relationships of aeolian erosion and deposition with LiDAR-derived landscape surface roughness following wildfire. *Geomorphology* **119**, 135–145. doi:10.1016/J.GEOMORPH.2010.03.013

Schmidtlein MC, Wood NJ (2015) Sensitivity of tsunami evacuation modeling to direction and land cover assumptions. *Applied Geography* **56**, 154–163. doi:10.1016/J.APGEOG.2014.11.014

Snyder GI (2012) The 3D elevation program: summary of program direction. US Department of Interior Geological Survey Fact Sheet 2012–3089. (Reston, VA, USA)

Soule RG, Goldman RF (1972) Terrain coefficients for energy cost prediction. *Journal of Applied Physiology* **32**, 706–708.

Tobler W (1993) Three presentations on geographical analysis and modeling. University of California at Santa Barbara, National Center for Geographic Information and Analysis Technical Report 93–1. (Santa Barbara, CA)

USDA Forest Service (2010) National wildland firefighter (NWFF) workforce assessment. (USDA Forest Service) Available at https://www.fs.fed.us/fire/management/assessments/phase1/NWFF_ReportPhaseI.pdf [Verified 20 December 2016]

USDA Forest Service (2014) First order LiDAR metrics: a supporting document for LiDAR deliverables. (USDA Forest Service, Remote Sensing Applications Center) Available at https://www.fs.fed.us/eng/rsac/LiDAR_training/pdf/LiDARMetricsDescriptionOfDeliverables_Generic_12_15_14.pdf [Verified 20 December 2016]

van Etten J (2015) gdistance: distances and routes on geographical grids. R package version 1.1–9. Available at http://CRAN.R-project.org/package=gdistance [Verified 20 December 2016]

Wood NJ, Schmidtlein MC (2012) Anisotropic path modeling to assess pedestrian-evacuation potential from Cascadia-related tsunamis in the US Pacific Northwest. *Natural Hazards* **62**, 275–300. doi:10.1007/S11069-011-9994-2

Ziegler JA (2007) The story behind an organizational list: a genealogy of wildland firefighters' 10 standard fire orders. *Communication Monographs* **74**, 415–442. doi:10.1080/03637750701716594